Primjena digitalne korelacije slike za separaciju modova kod loma kompozitne konstrukcije pri mješovitom opterećenju

Larma, Marijana

Master's thesis / Diplomski rad

2016

Download date / Datum preuzimanja: **2025-01-28**

UNIVERSITY OF ZAGREB

FACULTY OF MECHANICAL ENGINEERING AND NAVAL ARCHITECTURE

APPLICATION OF DIGITAL IMAGE CORRELATION TO DETERMINE MODE PARTITIONING IN MIXED-MODE FRACTURE OF COMPOSITE STRUCTURE

MASTER THESIS

Supervisors: Student:

Prof. dr. sc. Željko Tuković   Marijana Larma

Prof. dr. sc. Alojz Ivanković

Zagreb, 2016

Contents

Sveučilište u Zagrebu Fakultet strojarstva i brodogradnje	
Datum	Prilog
Klasa:	
Ur.broj:	

DIPLOMSKI ZADATAK

Student: **Marijana Larma**   Mat. br.: 0035177548

Naslov rada na hrvatskom jeziku: **Primjena digitalne korelacije slike za separaciju modova kod loma kompozitne konstrukcije pri mješovitom opterećenju**

Naslov rada na engleskom jeziku: **Application of digital image correlation to determine mode partitioning in mixed-mode fracture of composite structure**

Opis zadatka:

The use of fibre reinforced polymer-matrix composites extends to a wide range of industry sectors, due to their high specific strength and stiffness. The delamination toughness of such materials has been reported to be considerably dependent on the mode of loading. It is therefore important to carry out mixed mode tests so that the full failure locus ranging from mode I to mode II can be characterised. A number of analytical mixed mode partitioning theories exist in the literature that aim to predict the mode of loading in beam-like geometries as a function of beam height ratio and applied moment ratio. However, there is considerable disagreement between each analytical partitioning theory for asymmetric geometries and no analytical theory has been shown to be universally consistent with experimental findings.

A novel semi-analytical cohesive analysis (SACA) has been proposed based the observation that the normalised mode mixity is uniquely dependent on the normalised cohesive zone length, where the partitioning is bounded by the local partitioning of Hutchinson and Suo when there is zero damage length and the global partitioning of Williams if there is an infinitely large damage length. The mode mixity is calculated directly from the numerical simulations by applying the mode decomposed J integral, which requires the stress, strain and displacement field along an arbitrary path surrounding the damage zone.

In the scope of this thesis, digital image correlation will be used to directly determine the mode partitioning in standard asymmetric fixed ratio mixed mode (AFRMM) fracture tests on carbon fibre reinforced composite. Firstly, the method will be confirmed against known solutions for symmetric geometries and 3 different mode mixities. Secondly, the method will be applied to asymmetric geometries and compared against SACA.

It is advised to list references used in this work, as well as to acknowledge help and support possibly received during the course of this study.

Zadatak zadan: Rok predaje rada: Predviđeni datumi obrane:

14. siječnja 2016.   17. ožujka 2016.   23., 24. i 25. ožujka 2016.

Zadatak zadao: Predsjednik Povjerenstva:

Prof. dr. sc. Aloz Ivanković
Izv.prof. dr. sc. Željko Tuković   Prof. dr. sc. Tanja Jurčević Lulić

List of Figures

List of Tables

Nomenclature

DCB	Double Cantilever Beam
(A)FRMM	(Asymmetric) Fixed Ratio Mixed Mode
ELS	End Loaded Split
C-ELS	Calibrated End Loaded Split
DIC	Digital Image Correlation
NL	Non-Linear
PTFE	Polytetrafluoroethylene
SACA	Semi Analytical Cohesive Analysis
SD	Standard Deviation

Abstract

Composite materials combine two or more different materials, in order to obtain desirable properties. They are widely used in technical applications. The fracture mechanics of laminate composites display different behaviours than in monolithic materials, where mode I fracture is considered the critical case. This work is concerned with mixed modes of mode I and mode II fractures in laminate carbon fibre composite materials. Analytical partitioning theories on mixed mode fracture in composites show disagreements and no theory showed universal correspondence to experimental data. A semi-analitical cohesive zone analysis has been proposed by Conroy (Conroy, 2015) and the experimental data suggests good correspondence. In this thesis, digital image correlation is used with both standard tests on symmetrical samples and asymmetrical samples to produce different mode mixities, by varying the beam height ratio. Varying the beam height ratio makes it possible to perform tests with different mode mixities on standard testing machines, which are common in the industry as well. Tests were performed using a unidirectional composite manufactured from preimpregnated carbon fibre in epoxy resin. The samples have been speckled for DIC (Digital Image Correlation) and an open-source Matlab based code was used for the analysis of the images.

Extended Abstract (Croatian)

Kompoziti su materijali koji kombiniraju dva ili više materijala, s ciljem dobivanja poželjnih svojstava, naročito u pogledu specifičnih svojstava u odnosu na masu, zbog čega se primjenjuju primjerice kod letjelica ili lopatica vjetroturbina. Međutim, oni imaju i svoje nedostatke. Višeslojni kompozitni materijali skloni su delaminaciji. Delaminacija se događa kada pukotina počne rasti između dva sloja, što je uzrokovano uključinama zraka. Kao posljedica toga se višeslojni kompoziti ne ponašaju jednako pri lomu kao monolitički materijali.

Predstavljen je koncept modova pri lomovima materijala. čisti mod I se događa kada je pukotina opterećena normalno, na vlak. Mod II predstavlja smično naprezanje unutar ravnine, a mod III smično naprezanje izvan ravnine. Oni mogu opteretiti pukotinu u čistom obliku ili u kombinacijama moda I s jednim od druga dva u različitim omjerima. U ovom radu razmatrani su razni omjeri mješovitog moda I i II.

Za većinu inženjerskih materijala, mod I predstavljat će kritični slučaj, a pukotina će se izviti u mod I na vrhu. Slojevi kompozita predstavljaju ograničenje za to te će stoga pukotina nastaviti propagirati u mješovitom modu. U nekim slučajevima će se na taj način povisiti otpornost materijala na inicijalizaciju pukotine, a u nekima će se sniziti. Zbog navedenog se mod I ne može uzeti kao konzervativni slučaj i potrebno je istraživati ponašanje tih materijala pod opterećenjima različitih mješovitosti modova.

Razne analitičke teorije predlažu različite načine podjele modova. Možda su najznačajnije Williamsova (Williams, 1988), poznata kao globalna, i lokalna, koju su predložili Hutchinson i Suo (Suo & Hutchinson, 1990). Međutim, velika su neslaganja između teorija te se niti jedna postojeća analitička teorija ne podudara univerzalno s eksperimentalnim istraživanjima. S ciljem objedinjavanja eksperimentalnih ispitivanja, predložena je poluanalitička analiza kohezijske zone SACA (semi-analytical cohesive zone analysis) na osnovi numeričke analize koristeći model kohezijske zone. Eksperimentalni podaci sugeriraju učinkovitost i točnost ove metode.

Zrakaste geometrije uzoraka uspostavile su se najprikladnijima za eksperimentalno ispitivanje lomova. Varirajući omjer momenata na krakove i/ili omjer visina krakova, moguće je postići različite omjere modova. Mijenjajući omjer momenata, neposredno se može dobiti omjer modova, ali s obzirom na to da se ispitivanja s varirajućim visinama krakova mogu lako vršiti na standardnim strojevima za ispitivanja koja su učestala i u industriji, u interesu je uspostaviti metodu s kojom će biti moguće odrediti omjer modova za takva ispitivanja.

U sklopu ovog rada najprije su izvršena ispitivanja na simetričnim uzorcima sa standardnim testovima, a zatim na simetričnim uzorcima uz digitalnu korelaciju slika DIC (eng. Digital Image Correlation) te na asimetričnim uzorcima, varirajući mješovitost modova mijenjanjem omjera visina zraka uzorka (γ) uz DIC.

Ispitivanja vršena su na standardnom Tinius-Olsen stroju za ispitivanja, testnom metodom koja ima kontroliran vertikalni pomak, koji je za većinu testova iznosio 1 mm/min. U standardnim testovima na simetričnim uzorcima, pukotina se prati mikroskopom te kada dostigne označenu liniju zapisuje se vrijeme. Na osnovu tih podataka i izmjerenog dijagrama pomak - sila, računa se otpornost materijala za mod I - DCB (eng. double cantilever beam), mod II - ELS (end-loaded split) te mješoviti mod - FRMM (eng. fixed ratio mixed mode).

Za asimetrične uzorke je korištena metoda AFRMM (eng. asymmetric fixed ratio mixed mode), u kojoj je uzorak postavljen na isti način kao simetrični u FRMM metodi, s tim da su krakovi različite visine.

Kompozitni materijal te uzorci izrađivani su na licu mjesta, ručno. Za dobivanje višeslojnog kompozita, korišteni su slojevi predimpregriranih istosmjernih ugljičnih vlakana u epoksi smoli. Iz trake koja se drži na -18°C, kako može biti pohranjena do godinu dana, režu se listovi prethodno definirane veličine. Nakon odmrzavanja mogu se lijepiti jedan na drugi. Nakon dodavanja zaštitnih slojeva i brtvene trake, pripremljeni kompozit vakuumira se oko 45 minuta, te se stavlja u peć pod tlakom. Prvo se 40 minuta zagrijava do temperature od 110°C, na kojoj ostaje sat vremena, nakon čega temperatura ponovo raste do 180°C te se zadržava na njoj dva sata nakon čega se hladi prirodno. Kada se ohladi ispod 60°C, ukloni se pritisak, te se ostavlja da se hladi kako bi kompozitna ploča bila pogodne temperature za rukovanje. Tada se gotovi materijal reže u uzorke definirane veličine te se dodaju blokovi koji se pričvršćuju na aparat za testiranje.

Za određen broj uzoraka svih korištenih geometrija uzoraka primijenjena je metoda digitalne korelacije slike, za koju je bilo potrebno pripremiti uzorke sa sitnim česticama bijelog spreja na njihovoj crnoj površini, kako bi softver mogao pratiti istezanje površine na temelju točaka mreže koja se odredi za korelaciju. Za tu analizu korišten je program otvorenog koda. Grafički su prikazani pomaci i istezanja.

Chapter 1

Introduction

1.1 Composites

Composite materials combine two or more different materials, in order to obtain desirable properties, especially high strength-to-weight and stiffness-to-weight ratios, which are essential in the aircraft and spacecraft industry. In addition, they are cost-effective. There is evidence of composite material usage throughout history, with examples of plywood in ancient Egypt and straw for strengthening mud bricks in ancient Israel (Jones, 1998). The goal in most cases is to obtain certain properties existent in each of the compound materials, but in some cases new properties can be created that arise solely from the combination (Quan & Ivanković, 2015). In this work, the focus is on long fibre polymer matrix composites, precisely carbon fibre reinforced polymer matrix (CFRP). Carbon and Glass (CFRP and GFRP) are the most common long fibres used for this. They are high moduli and high strength and provide strength and stiffness, which are significantly higher than the bulk material, due to the fact that they are only 5-10 μm thin, allowing the crystals to align in an ordered structure, that causes much less possibilty for defects than bulk material (Gordon, 1991). In Figures 1.1 and 1.2 some typical applications of composite materials are represented.
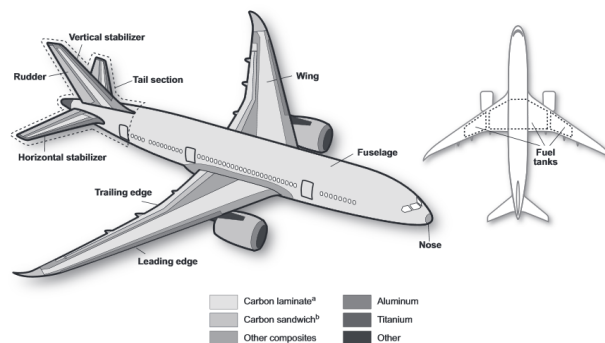
Figure 1.1: Different types of composites applied in aircrafts (GAO-11-849)

Figure 1.2: Glass fibre reinforced composite in wind turbine blades (the, 2016)

1.2   Fractures in Composite Materials

Firstly, the concept of fracture modes shall be introduced. There is three pure modes of loading a crack. Mode I corresponds to a tensile stress, normal to the crack plane. Mode II refers to an in-plane shear stress and Mode III is an out-of-plane shear stress. These modes can occur to a crack as pure modes or in combinations of two modes. The three modes are visualized in Figure 1.3 (Murphy, 2015).
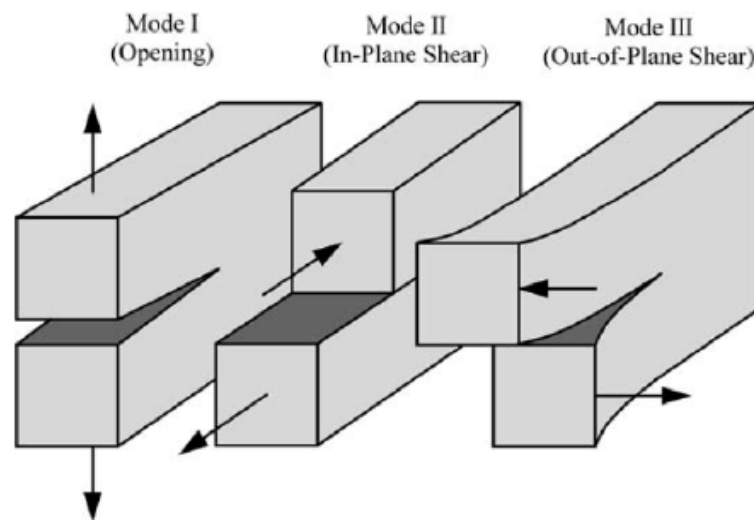
Figure 1.3: Graphical representation of the pure modes on a crack (Anderson, 2005)

In brittle engineering materials, most often mode I will be the most critical. Tests for mode I, along with other tests on symmetric specimens, can performed on standard testing machines and are straightforward. For these, beam-like geometries have been found convenient as the total energy release rates, commonly used for characterising the mode mixity, can be easily extracted using simple beam theory (Williams, 1988). A beam-like geometry used for fracture testing is shown in Figure 1.4.
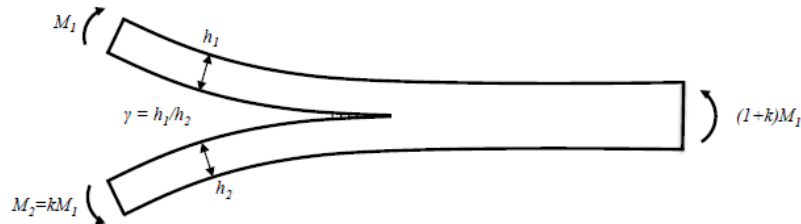
Figure 1.4: Beam-like geometry for fracture testing (Conroy, 2015)

Varying mode mixities can be achieved in different ways. The FRMM test with the symmetric samples has a fixed ratio of $G_{II}/G = 3/7$. For obtaining other ratios, either beam height ratio, γ, or the applied moment ratio, k, can be varied. For varying k requires specific equipment, whereas specimens with different beam height ratios can be tested on standard testing machines, but in this case it is less straightforward to determine the mode I and mode II energy release rates.

Pure mode I tests are practiced in the industry as well, also for composite materials, as they are considered the critical case, as a mixed mode crack will deviate to mode I at the crack tip (Cotterell & Rice, 1980). For laminate materials though, this has proven to not always be the case. If the crack propagates between the plies, it will be forced to propagate as a mixed mode crack and sometimes display a higher, or a lower initiation toughness (Dillard *et al.*, 2009).

In this work, the concern will be different mixities of mode I and mode II.

Several analytical partitioning theories have been proposed. Perhaps the most important ones by Williams (Williams, 1988), referred to as the global partitioning theory and by Hutchinson and Suo (Suo & Hutchinson, 1990), commonly called the local partitioning theory. There is great disagreements between analytical theories, and while each theory coincides with a certain case, experimental analyses have shown that no one of them can predict failure loci in the general case. A semi-analytical cohesive analysis has been proposed by Conroy, based on numerical analysis using cohesive model, which seems to be supported by the experimental data (Conroy, 2015).

Chapter 2

Material and Specimen Preparation

2.1 Composite Manufacturing

The composites for the specimens are manufactured in University College Dublin from pre-impregnated carbon fibres using a vacuum bagging procedure and a pressclave. The material used for this thesis is a uni-directional AS4/8552 (carbon/epoxy) composite (Hex, 2016). The prepreg tape has a nominal fibre volume of 57%. The matrix HexPly® 8552 is a tough epoxy matrix used primarily in aerospace structures, due to its high performance and good impact resistance and damage tolerance. The benefits and features of the matrix are:

- Toughened epoxy matrix with excellent mechanical properties

- Elevated temperature performance

- Good translation of fibre properties

- Controlled matrix flow in processing

- Available on various reinforcements

- Excellent drape and tack

The composite is delivered as a pre-impregnated roll of 45 meters and stored in a freezer at -18°C. In the freezer it has a shelf life of 12 months. The tack life is 10 days, which means after being taken out of the freezer the layup has to be done within that period. Altogether, after the removal from the freezer it is allowed to stay at room temperature for up to 30 days before the curing process.

2.1.1 Layup Procedure

The prepreg tape is removed from the freezer to cut sheets of the required size, depending on the number and the dimensions of the desired test specimens. It was found to be easier to cut sheets of the right size off the roll right after removing it from the freezer, while they are less deformable. The sheets are cut using a stanley knife and a square ruler. The plies are then left outside the freezer overnight. The following day they are layed up on top of each other by hand one by one with the fibres aligning in the 0° direction. The total thickness for the symmetric samples in each case was 3.9 mm, with the precrack teflon film placed at the midplane. As the nominal cured thickness of a prepreg ply is 0.15 mm, this results in a layup of 13/13 layers. Between the 13th and the 14th layer the crack starter film is placed, which is a very thin PTFE film, only 13 μm in thickness and it simulates a physical precrack. It is placed so that after cutting the length of the inserted film is 57.5 mm for the mode 1 and mixed mode samples (45 mm from the load line) and 67.5 for the mode 2 samples (55 mm from the load line). For the asymmetric samples, the choice of the beam height ratios resulted in using a total of 28 layers where the crack starter film was placed according to the desired mode mixity. The beam height ratios are shown in Table 2.1.

Table 2.1: Beam thicknesses of the asymmetric samples

l [mm]	h_t [mm]	h_1 [mm]	h_2 [mm]	γ	No. of repeats
190	4.2	1.35	2.85	0.47	3
190	4.2	2.7	1.5	1.8	3
190	4.2	3.15	1.05	3	3
190	4.2	3.45	0.75	4.6	3

The corresponding number of layers is 9/19 ($\gamma = 0.47$), 18/10 ($\gamma = 1.8$), 21/7 ($\gamma = 3$) and 23/5 ($\gamma = 4.6$). The crack starter film is again placed in a way that the insert is 67.5 mm (55 mm from the load line) in all the cut samples except for $\gamma = 0.47$, where the insert length is 57.5 (45 mm from the load line). The layup is placed on the base plate, protected by PTFE sheets on both sides. The PTFE sheets enable removing the layup from the base plate after debulking and keep the surfaces of the uncured layup clean. The

layup and the PTFE sheets are placed so that they do not cover the holes for the vacuum. A breather is placed over the layup and the vacuum holes to ensure the vacuum over the plate. It is closed off with a bagging film and sealant tape. After making sure there are no leaks between the sealant tape and the bagging film, the vacuum pump is left on for debulking for 45 minutes.

The layup is debulked to help eliminate air pockets between the layers and ensure the laminate is consolidated. If the debulking process is skipped, voids may appear which can lead to impaired mechanical properties (i.e. delamination resistance) of the produced composite panels. (Mohan, 2010) An exploded view of the debulking layup is shown in Figure 2.1.
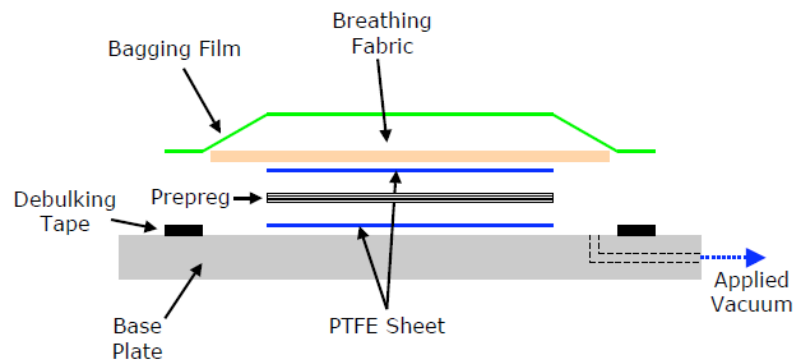

Figure 2.1: Exploded view of the debulking layup

Figure 2.2: Debulking vacuum check

2.1.2   Layup Procedure

After the debulking, the layup is prepared for the curing process. A new PTFE film is placed on the base plate of the mould. Right under and over the laminate, a film of release ease is added to help provide a consistent surface finish on the top and bottom of the cured composite. Another PTFE film is layed on top of it. Edge dam tape is placed around the layup to prevent the resin from leaking. A rubber pad helps to evenly distribute the downward pressure in the pressclave. None of this should cover the vacuum holes, as opposed to the breathing fabric that is placed next. Again a bagging film is closing off the layup, this time with high temperature sealant tape all around it. Another time the vacuum is checked for leaks. A high temperature sealant tape is also applied on the edges of the base plate to seal the base plate and the top lid together. The exploded view of the layup for curing can be seen in Figure 2.2.

For the curing process, both pressure and temperature are required.

For this, a hydraulic press was converted into a pressclave in UCD by installing heaters and a temperature control system. (Mohan, 2010)

Firstly, the mould is mounted inside the pressclave and the safety block is removed to enable lowering the hydraulic press. It is lowered onto the top lid and a 30 ton force is applied. Then the pressurized air is introduced though a tube between the top lid and the bottom plate, creating a pressure chamber, necessary for consolidating the laminate during the curing process. The vacuum pump is switched on to create a vacuum under the bagging film. Finally, the curing process is set and the heaters are switched on. The temperature is programmed to follow the recommended curing cycle:

- heat to 110°C over a period of 40 minutes

- hold at 110°C during 60 minutes

- heat to 180°C over a period of 30 minutes

- hold at 180°C during 120 minutes

- hold at 180°C during 120 minutes

- cool at rate 0.1 - 1 °C per minute

For the cooling there is no special system, the heaters are simply switched off and the plates are air-cooled.

During the curing the window must be open and the air ducts must transport the hot air outside, as shown in Figure 2.3.
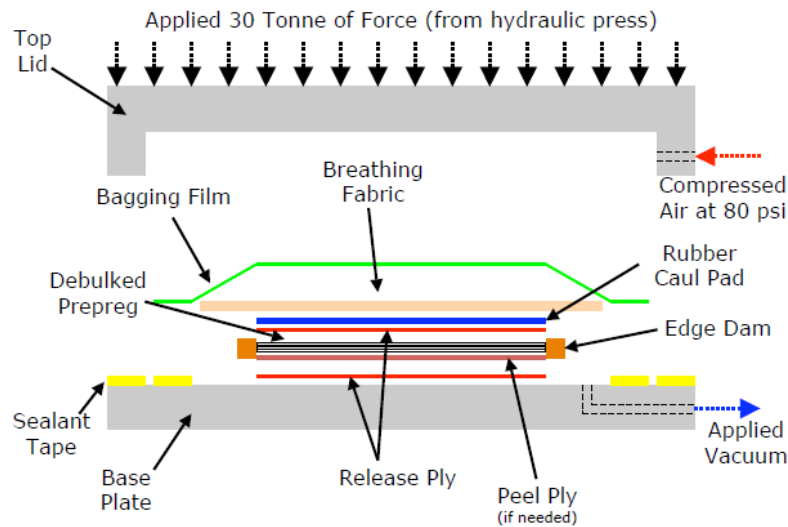
Figure 2.3: Exploded view of the curing layup

It takes about 4-5 hours after the heaters are switched off (which happens automatically after the cycle has finished) for the temperature in the mould to fall below 60°C. When this has happened, the pressure can be turned off. Firstly the vacuum pump is switched off, then the pressure in the chamber is reduced to atmosphere pressure and finally the pressclave is switched off. The system is then left to cool overnight to enable handling mould and the material. After the unit is removed from the pressclave, the top lid has to be lifted off the base plate by removing and cutting the outer sealant tape. Then the other tapes and sheets are removed to take out the cured composite plate.

Figure 2.4: Pressclave

2.2   Preparation of the Specimens

After curing and cooling, the plate is cut under a fume hood using a diamond grinding disc. The disc width is 2.5 mm and has to be taken into account when planning the number of specimens. The reference line is the crack starter film that is left a bit outside of the laminate to determine its position. From there parallel and perpendicular lines are made to cut along. Precautions are taken to try to prevent the carbon fibre sawdust to enter the lungs and the skin. After the cutting, the specimens are cleaned with paper towels and load blocks are glued to them according to the test method used for the sample. All of the symmetric samples are 3.9 mm thick and 25 mm wide. The width is 190 mm for fixed ratio mixed mode and end loaded split and 150 mm for double cantilever beam. The asymmetric samples are all 190 mm in length, 25 mm in width and 4.2 mm in thickness. The load blocks are attached with glue according to the test method. For DCB there are two load blocks, one on each side of the crack opening. For FRMM there is one on top and for ELS there is one on the bottom. The surfaces to be observed either with the microscope or for DIC are polished with fine sandpaper. For the standard methods, a thin layer of white water-based paint is applied before marking the distance lines with a 0.5 mm fine liner. For the DIC, a fine pattern of white spray paint particles is sprayed onto the black surface of the specimen. To achieve this fine pattern, several attempts with different types of spray paint, directions and distances were done. To see whether the speckles are in the right size range, a microscope is used with a length reference next

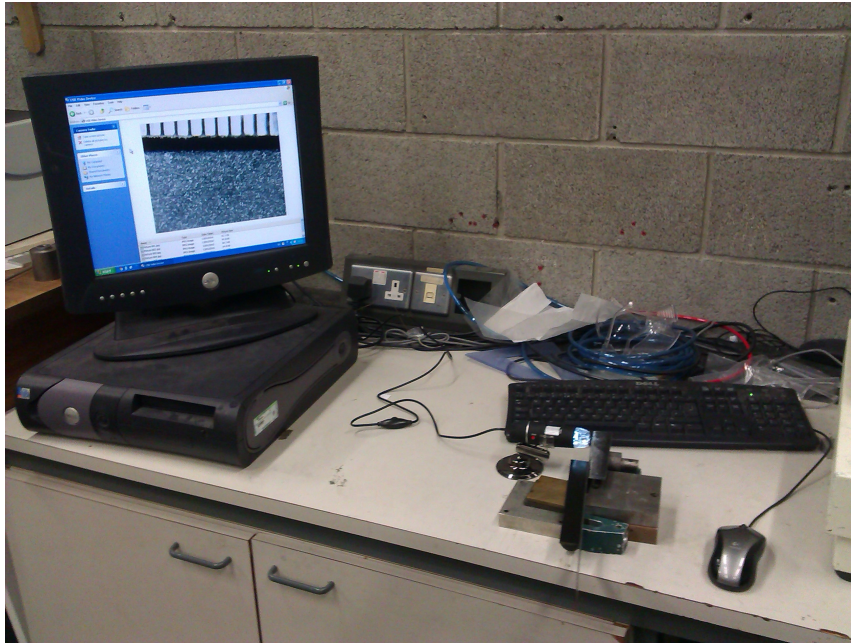to the sample as shown in Figure 2.5.

Figure 2.5: Speckle size check

Chapter 3

Experimental Setup

3.1 Standard Test Methods

The standard tests are performed on the symmetric samples with a screw-driven Tinius-Olsen testing machine with a 10 kN load cell. The same programmed test method is used for all the tests, which is a displacement-controlled method with a steady upward motion of the load cell attached to the load block, at 1 mm/min. The rigs for the tests with the symmetric samples can be seen in Figure 3.1. A travelling microscope is installed in front of the machine to follow the crack tip during the tests. When the crack tip hits a mark, the time is noted, which is later used in the delamination toughness calculation. At the same time, the load-displacement curve is recorded. To create a more physical crack tip, the samples are firstly precracked until the first 5 mm. The FRMM and ELS samples are also precracked in mode I, as they tend to initialize in an unstable manner. Before the actual mode II and mixed mode tests, the additional load block used for precracking the samples in mode I is removed. Four specimens were tested in the FRMM test, and three in each the DCB and the ELS tests. Equations (3.1), (3.2) and (3.5) show how the fracture toughnesses were calculated. The initiation values were obtained using the Max/C0-5%/NL point, as defined in (ISO 15024:2001). All the tests are performed according to the standrads (ISO 15024:2001), (ISO 15114:2014), (Blackman *et al.*, 2001).

(a)
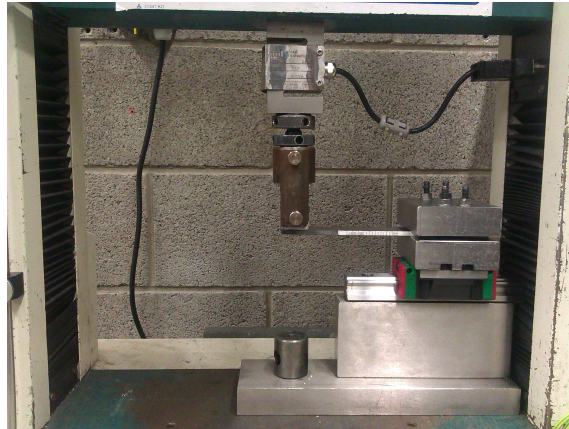
(b)
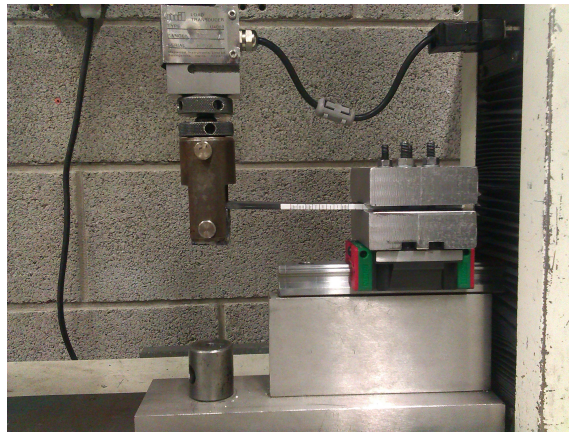
(c)

Figure 3.1: Load vs. crosshead displacement for asymmetric fixed ratio mixd mode (AFRMM) samples

The data required for the calculations is:

- ω - initial delamination length

- a - total delamination length ($a = a_0$+measured delamination length increments)

- P - load

- δ - load line displacement

- C - load line compliance δ/P

- b - width of specimen

- $2h$ - thickness of specimen

$$DCB \implies G_{IC} = \frac{3P\delta}{2B(a + |\Delta_I|)} \cdot \frac{F}{N} \tag{3.1}$$

$$FRMM \implies G = G_I + G_{II} \tag{3.2}$$

$$G_I = \frac{3P^2(a + \Delta_I)^2}{B^2 Eh^3} \cdot \frac{F}{N} \tag{3.3}$$

$$G_{II} = \frac{9P^2(a + \Delta_{II})^2}{4B^2 Eh^3} \cdot \frac{F}{N} \tag{3.4}$$

$$C\text{-}ELS \implies G_{IIC} = \frac{9P^2(a_e)^2}{4B^2 Eh^3} \cdot \frac{F}{N} \tag{3.5}$$

Where:

- F is the large-displacement correction

- N is the load block correction

- E is the substrate exural or tensile modulus

- Δ_I and Δ_{II} are correction factors for root rotation of the crack tip

For the ELS specimens, it is difficult to track the crack propagation with the travelling microscope as it is not as clearly recognizable. For obtaining the toughness values, the CBTE method is used (Corrected Beam Theory with Effective Crack Length), as it is independent of measured crack length. This requires performing the calibration of the ELS fixture and the determination of the ELS clamp correction. The calibration is performed by fixing an uncracked sample with the crack fully inside the clamp with a varying free length of 50, 60, 70, 80, 90 and a 100 mm and loading it elastically until 250 N and unloading. In all the applications of the clamp, reproducibility is achieved by tightening the nuts to the same level with a torque wrench, precisely 8 Nm by recommendation.

Figure 3.2: Tightening of the clamp using a torque wrench

The determination of the clamp correction is calculated as follows:
Firstly, for each free length the Compliance (C) is obtained by linear regression, ignoring any initial non-linearity due to take up. Secondly, the $C^{1/3}$ is plotted against L. Another linear regression is performed, extending to $C^{1/3} = 0$. From the slope of this line the flexural modulus of the specimen, E_1, is calculated. The intercept value at the L-axis is the clamp correction, Δ_{clamp}. The Compliance of the system is written as in Equation 3.6, where the effective crack length is taken from, as expressed in Equation 3.7 (ISO 15024:2001).

$$C = \frac{\delta}{P} = \frac{3(a_e)^3 + (L + \Delta_{clamp})^3}{2bh^3 E_1} \qquad (3.6)$$

$$a_e = \left[\frac{1}{3} \left\{ 2bCh^3 E_1 - (L + \Delta_{clamp})^3 \right\} \right]^{\frac{1}{3}} \qquad (3.7)$$

3.2   Digital Image Correlation

For the digital image correlation, a digital single-lens reflex camera with 18 megapixels was mounted on a tripod and zoomed in as close as it is allowed to focus. It is then set to take pictures continuously, at 150 frames per minute (this was the technical limit, using sensitivity setting of ISO 100), with an aim to capture the moment as close as possible to the crack initiation. A led lamp is used for lighting, as by heating the material (e.g. by a strong reflector) its properties change with the temperature rise. The setup can be seen in Figure 3.3. Figure 3.4 shows an attempt to focus the lens correctly.

Figure 3.3: Setup of the DSLR at the testing machine

The software used is an open-source Matlab-based GUI. It is based on a DIC code written by Christoph Eberl, et. al. at the John Hopkins University, modified by Elizabeth Jones, University of Illinois. (Jones, 2013).

DIC is a method that uses characteristic surface points on a grid to track the deformation of the material this is why the stochastic pattern of a fine speckle is applied prior to testing. The software follows the grid points and gives information about the displacements and the strain - given a measure of length per pixel.

Figure 3.4: Focusing the lens on the speckled sample

3.2.1 Symmetric Samples

Firstly, a sample of each type of symmetric samples was tested using this method, using the same setup as in Figure 3.1, but with samples prepared for DIC with white spray paint (see Figure 3.5).
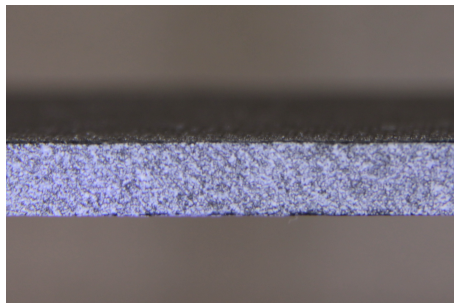
Figure 3.5: An uncracked speckled sample for DIC

3.2.2 Asymmetric Samples

The beam thicknesses of the asymmetric samples are as outlined in Chapter 2. The method used is AFRMM (Asymmetric Fixed Ration Mixed Mode), with the same test rig as in the FRMM with the symmetric samples, one load block on top - pulling one beam upwards. The load-displacement graphs are recorded as for the previous tests.

Chapter 4

Results

4.1 Symmetric samples

The results from the standard tests with the symmetric samples are outlined in the following figures. Figure 4.1 presents the results from DIC, Figure 4.2 shows FRMM and Figure 4.3 ELS.

Table 4.1: Average initiation toughness values (G_c) and standard deviation (SD) for mode I DCB tests from precrack

DCB	G_c, [J/m^2]	SD
Specimen 1	245.92	6.12
Specimen 2	225.10	10.58
Specimen 3	238.90	13.79

Table 4.2: Average initiation toughness values (G_c) and standard deviation (SD) for FRMM tests from precrack

FRMM	G_c, [J/m^2]	SD
Specimen 1	352.62	17.10
Specimen 2	331.78	27.02
Specimen 3	332.29	37.40
Specimen 4	317.03	20.69

Table 4.3: Average initiation toughness values (G_c) and standard deviation (SD) for ELS tests from precrack

ELS	G_c, [J/m^2]	SD
Specimen 1	646.15	6.80
Specimen 2	590.98	11.85
Specimen 3	577.83	13.17

For the ELS samples, the calibration was performed as described in Chapter 3. In Figure 4.1. the cube root of the Compliances obtained from the calibration are plotted against the free length. The linear regression with the intercept is shown in Figure 4.2. The values calculated from this are presented in Table 4.4.
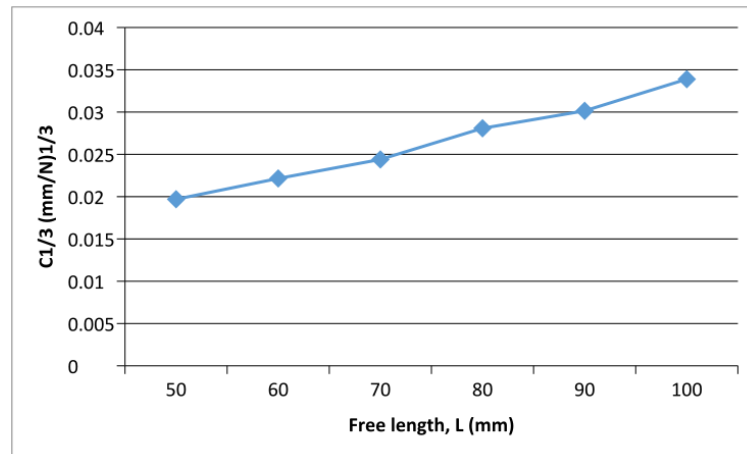
Figure 4.1: Clamp calibration data
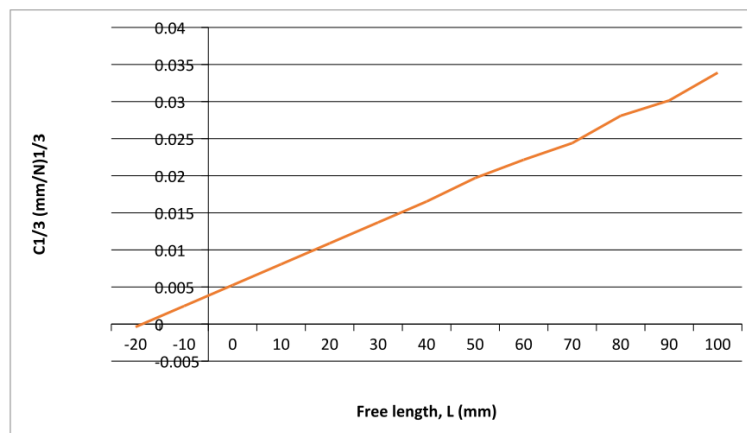
Figure 4.2: Linear regression of calibration data

Table 4.4: Values obtained from clamp calibration.

E_1 [Pa]	1.2039E+11
Δ_{clamp} [m]	0.01797888

4.2 Digital Image Correlation

The results obtained from the Digital Image correlation are presented in the following figures.

4.2.1 Symmetric samples

For each test method, three tests were performed. The ones that correlated best are shown in the figures.

DCB sample
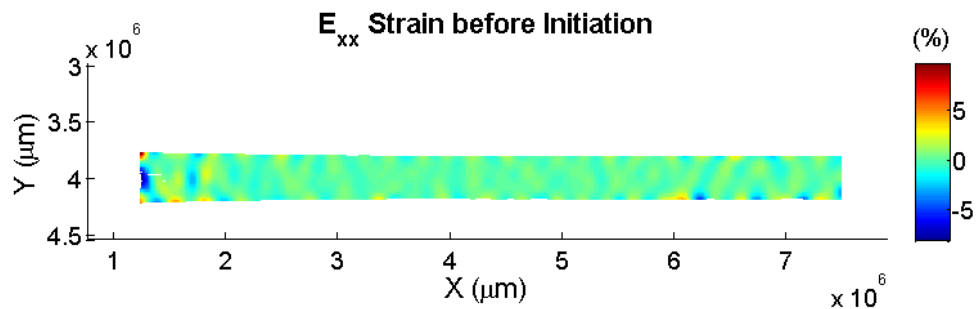
Figure 4.3: Computed E_{xx} strain before crack initiation - DCB sample
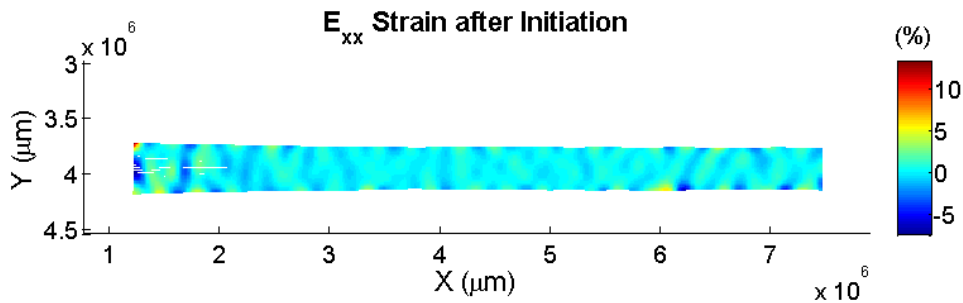
Figure 4.4: Computed E_{xx} strain after crack initiation - DCB sample
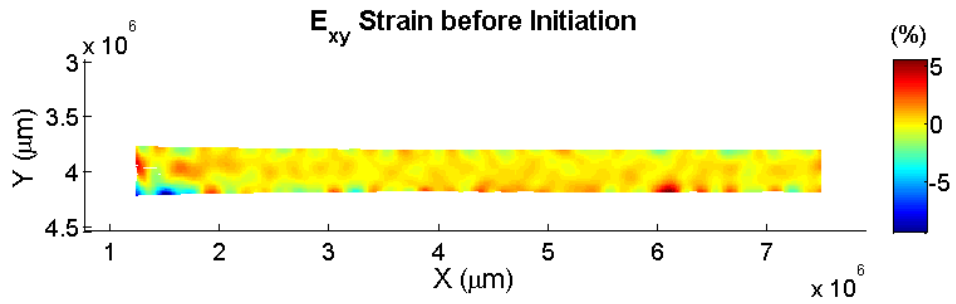
Figure 4.5: Computed E_{xy} strain before crack initiation - DCB sample
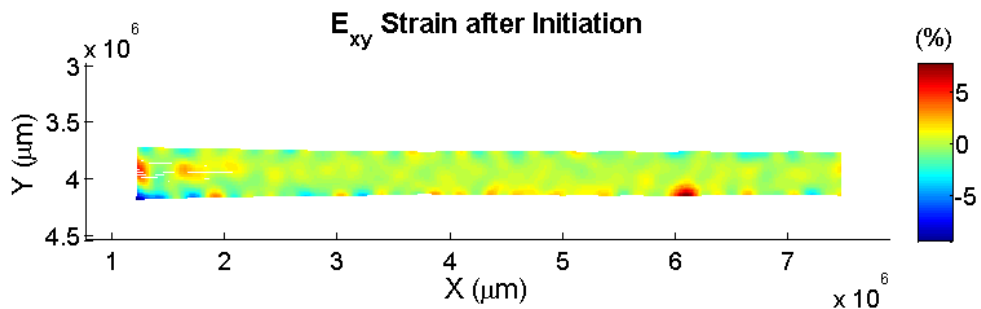
Figure 4.6: Computed E_{xy} strain after crack initiation - DCB sample
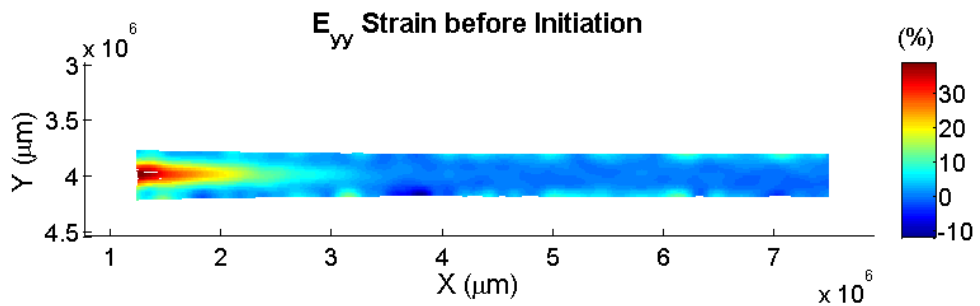
Figure 4.7: Computed E_{yy} strain before crack initiation - DCB sample
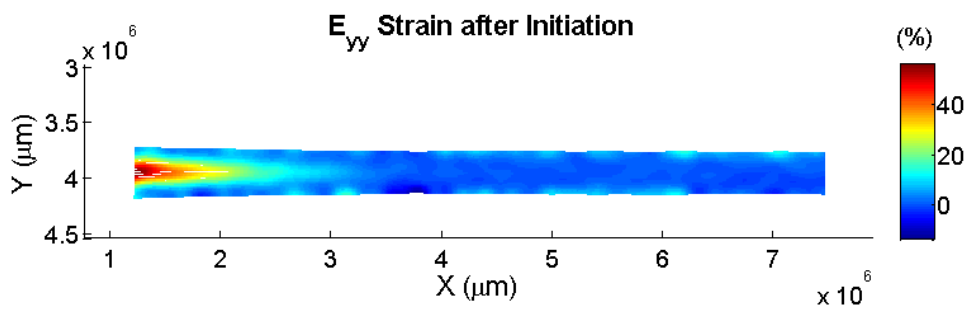
Figure 4.8: Computed E_{yy} strain after crack initiation - DCB sample
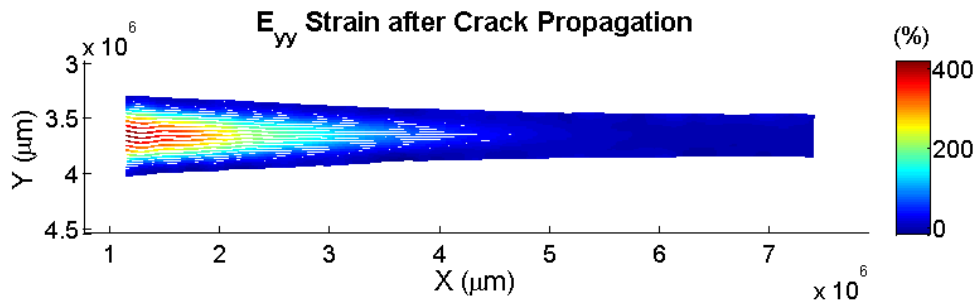
Figure 4.9: Computed E_{yy} strain after propagation - DCB sample
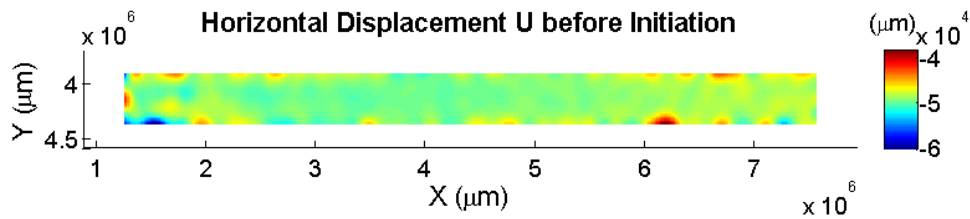
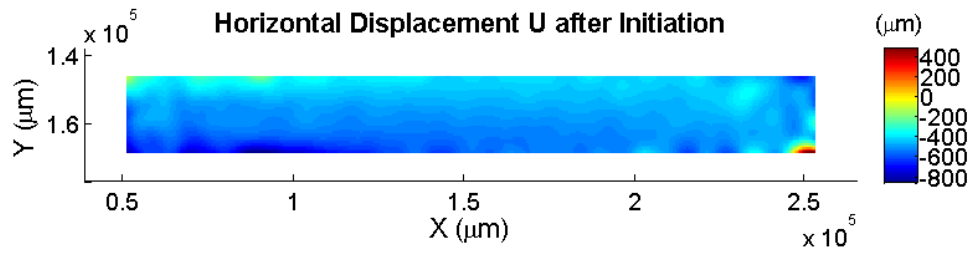Figure 4.10: Computed horizontal displacement U before crack initiation - DCB sample
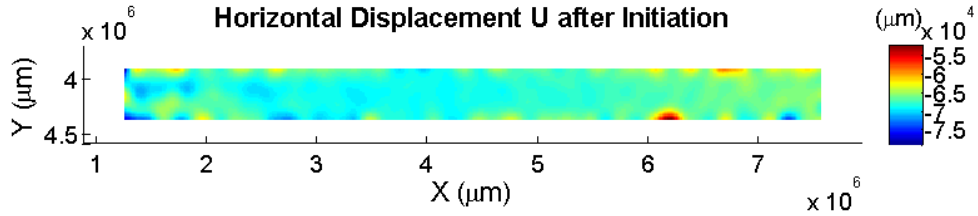
Figure 4.11: Computed horizontal displacement U after crack initiation - DCB sample
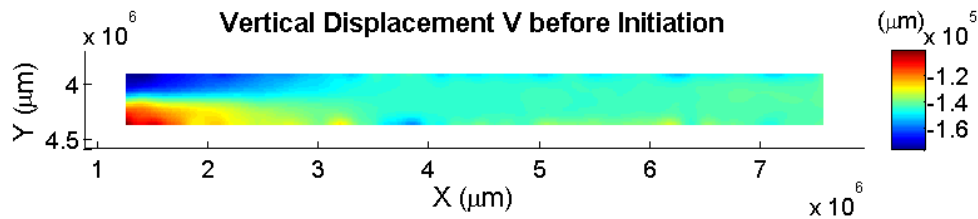
Figure 4.12: Computed vertical displacement V before crack initiation - DCB sample
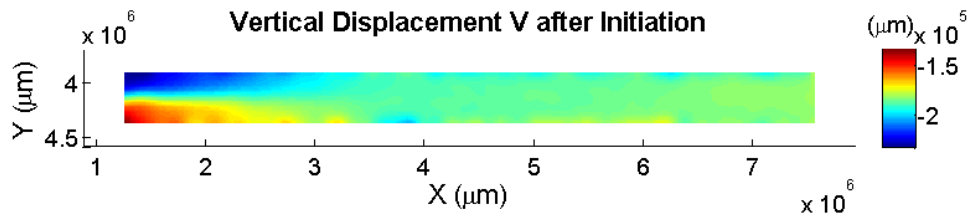
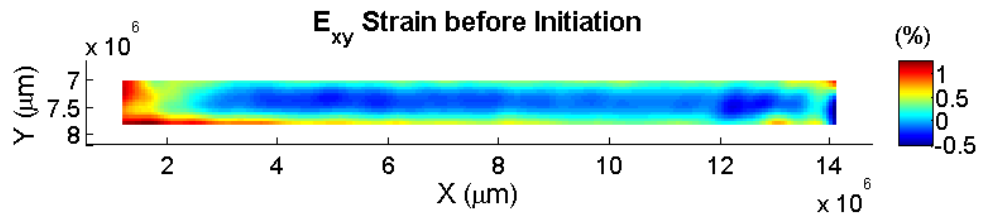Figure 4.13: Computed vertical displacement V after crack initiation - DCB sample
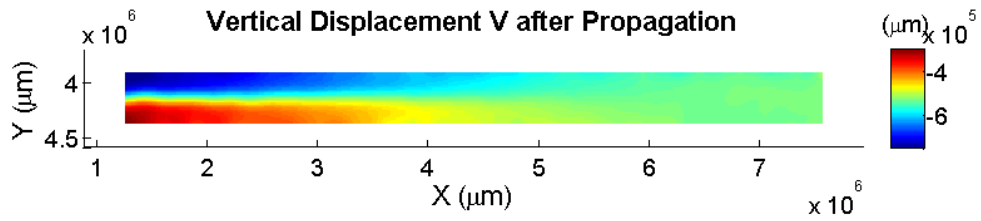
Figure 4.14: Computed vertical displacement V after crack propagation - DCB sample
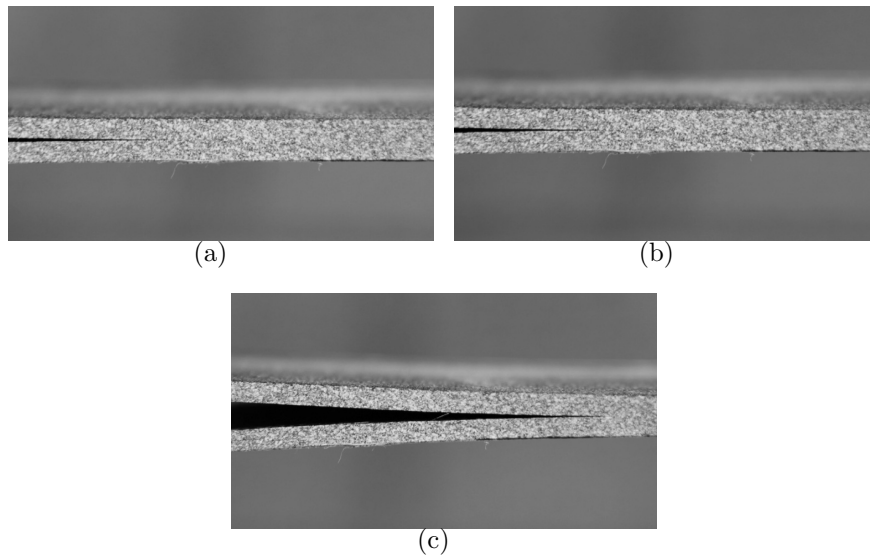
Figure 4.15: Frame before initiation (a). Frame after initiation (b). Frame after propagation (c).

FRMM sample
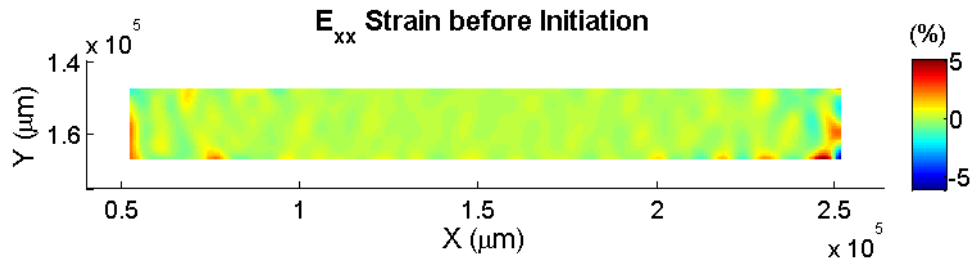
Figure 4.16: Computed E_{xx} strain before initiation - FRMM sample
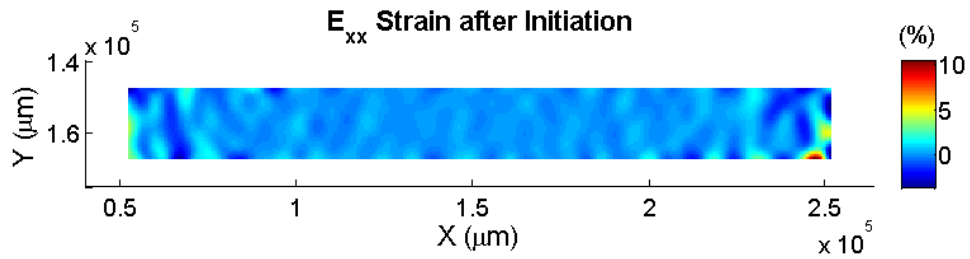
Figure 4.17: Computed E_{xx} strain after initiation - FRMM sample
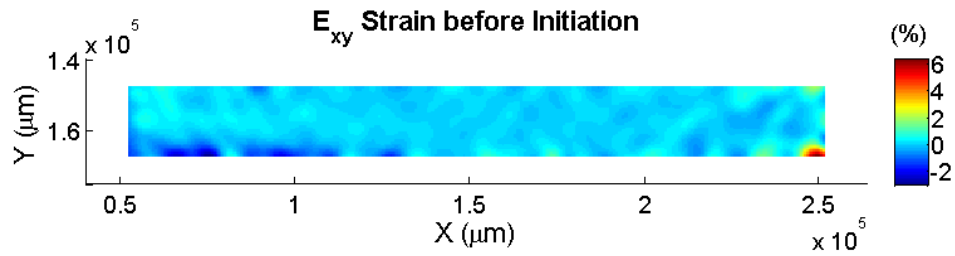
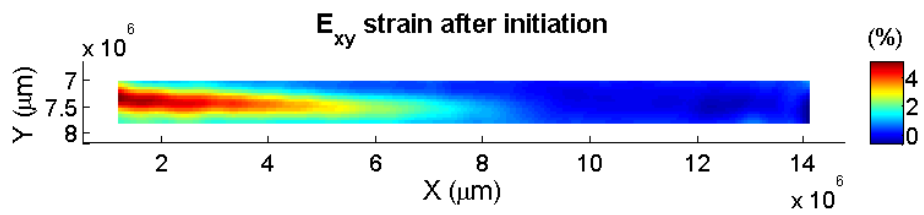Figure 4.18: Computed E_{xy} strain before crack initiation - FRMM sample
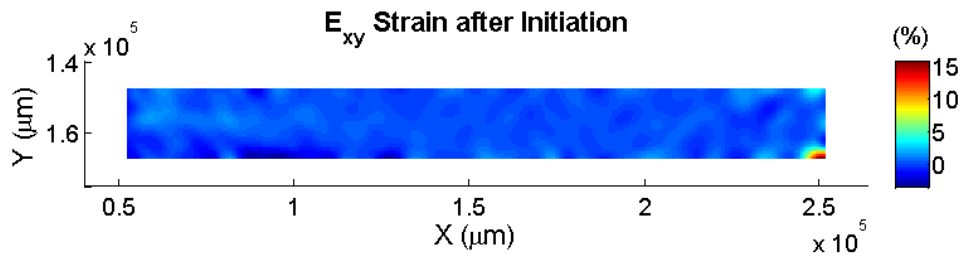
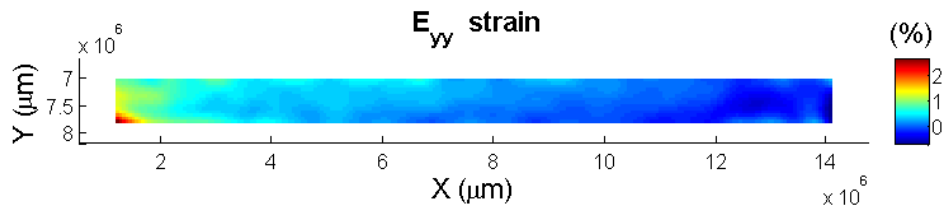Figure 4.19: Computed E_{xy} strain after crack initiation - FRMM sample
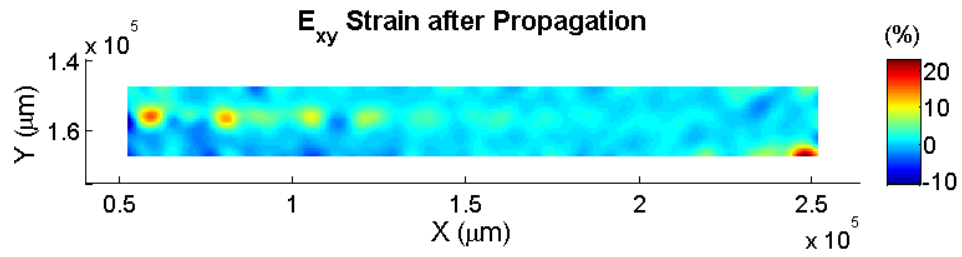
Figure 4.20: Computed E_{xy} strain after crack propagation - FRMM sample
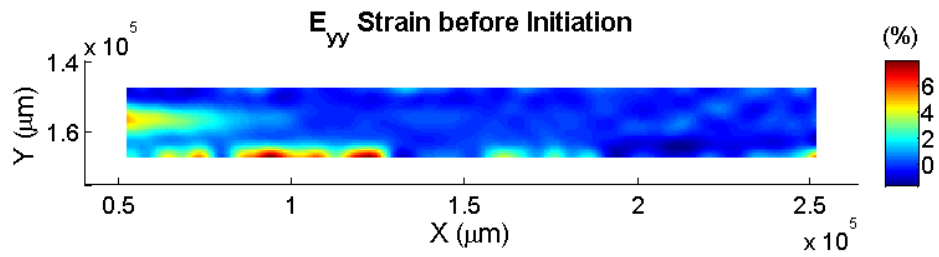
Figure 4.21: Computed E_{yy} strain before crack initiation - FRMM sample
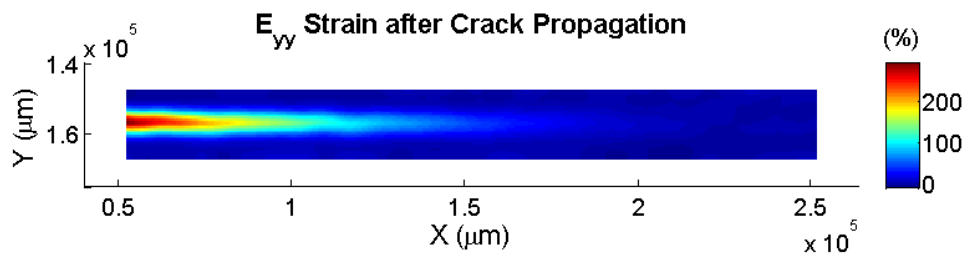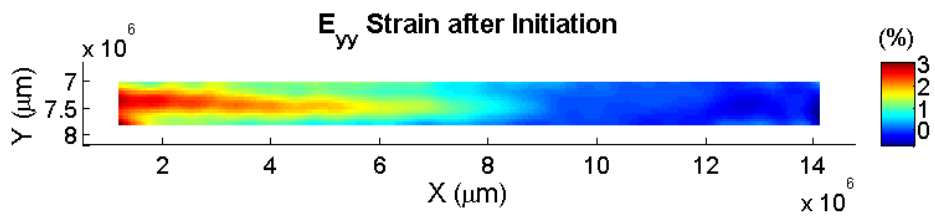

Figure 4.22: Computed E_{yy} strain after crack propagation - FRMM sample
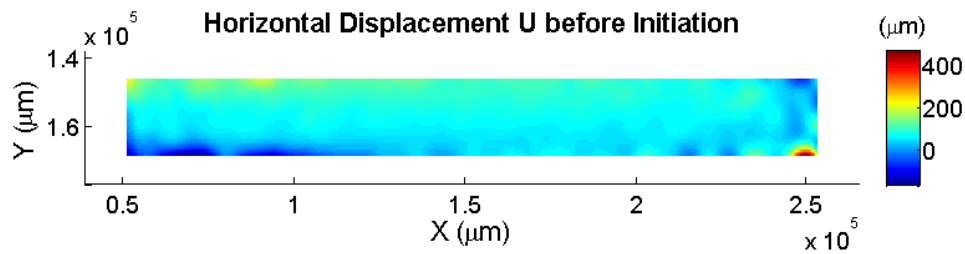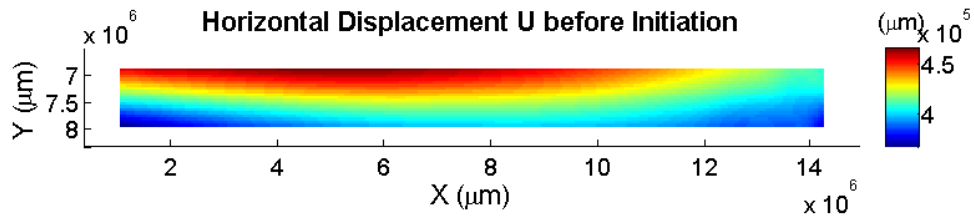

Figure 4.23: Computed horizontal displacement U before crack initiation - FRMM sample
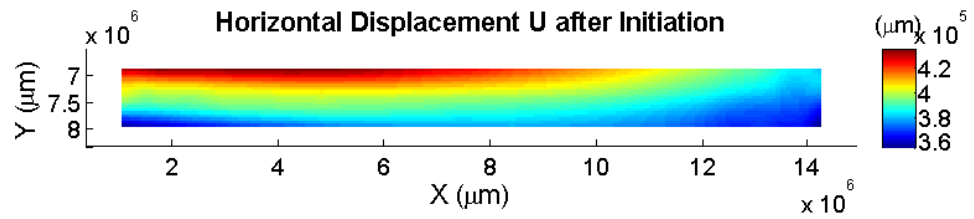
Figure 4.24: Computed horizontal displacement U after crack initiation - FRMM sample
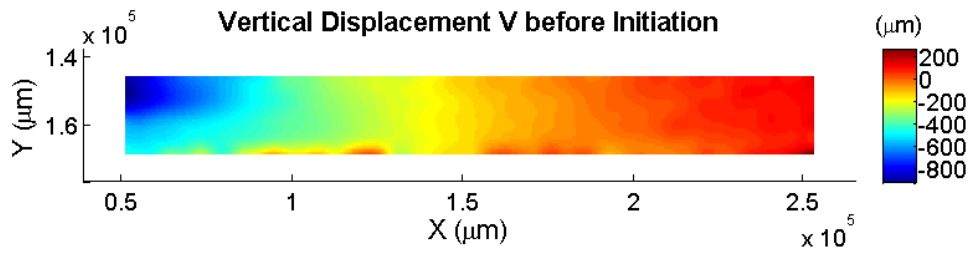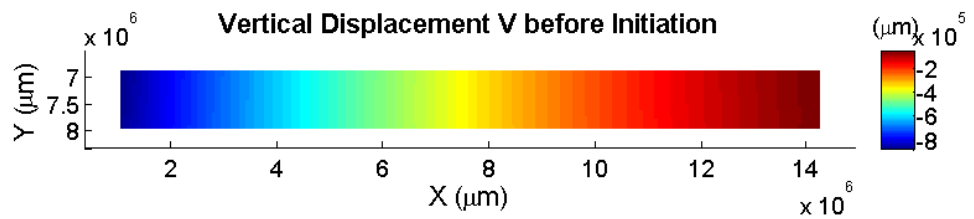

Figure 4.25: Computed vertical displacement V before crack initiation - FRMM sample
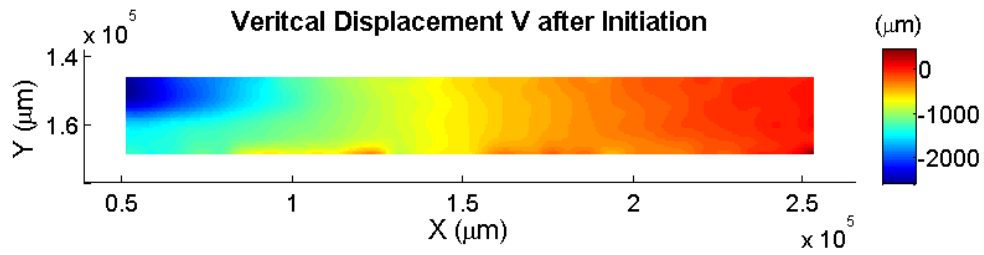
Figure 4.26: Computed vertical displacement V after crack initiation - FRMM sample
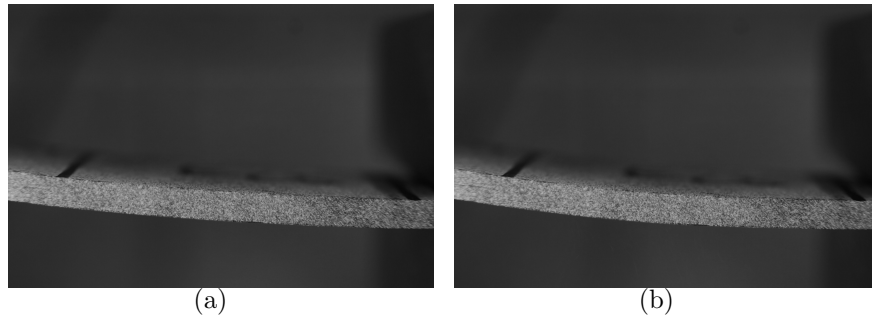
(a)

(b)

(c)
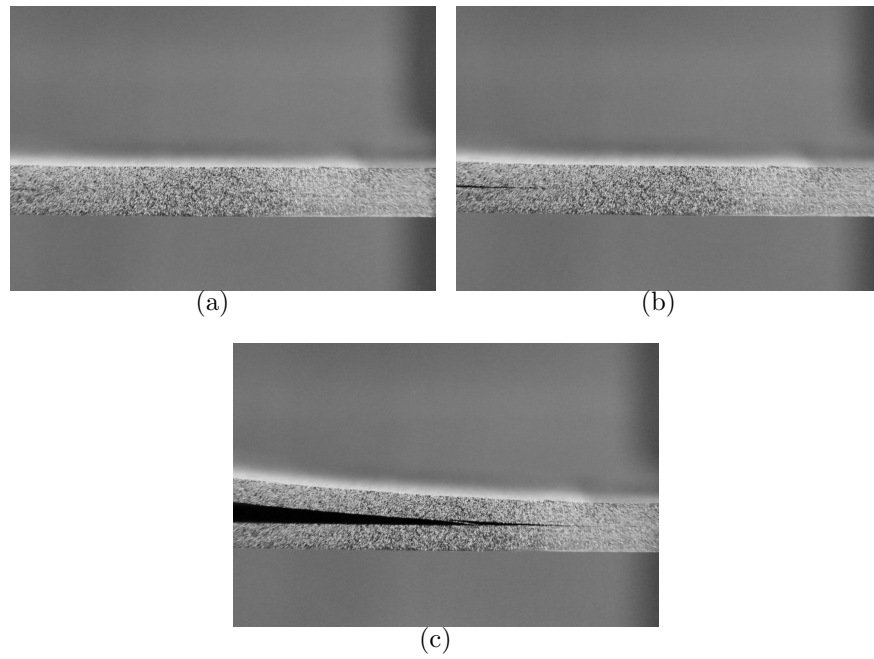
Figure 4.27: Frame before initiation (a). Frame after initiation (b). Frame after propagation (c).

ELS sample
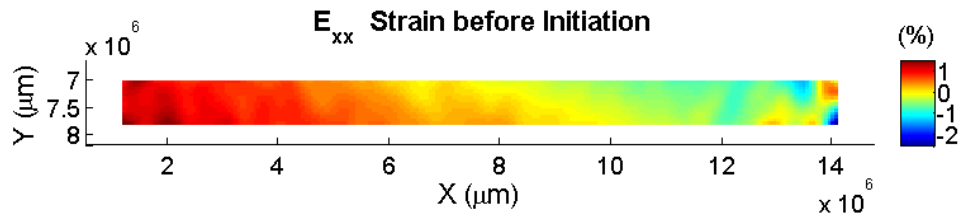
Figure 4.28: Computed E_{xx} strain before crack initiation - ELS sample
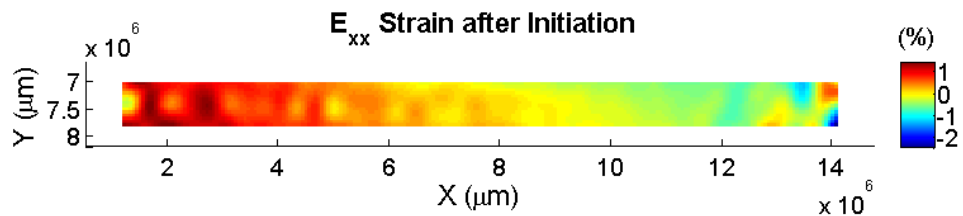
Figure 4.29: Computed E_{xx} strain after crack initiation - ELS sample
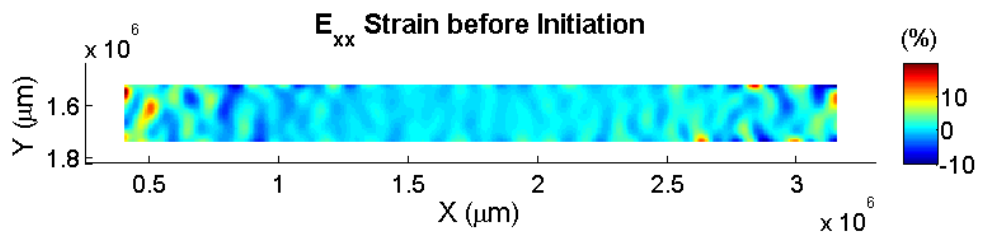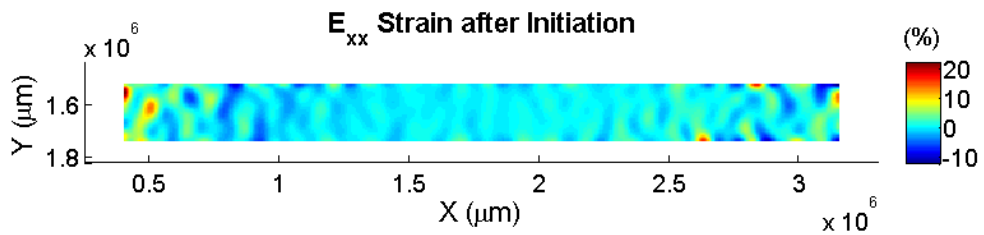
Figure 4.30: Computed E_{xy} strain before crack initiation - ELS sample

Figure 4.31: Computed E_{xy} strain after crack initiation - ELS sample

Figure 4.32: Computed E_{yy} strain before crack initiation - ELS sample

Figure 4.33: Computed E_{yy} strain after crack initiation - ELS sample

Figure 4.34: Computed horizontal displacement U before crack initiation - ELS sample

Figure 4.35: Computed horizontal displacement U after crack initiation - ELS sample

Figure 4.36: Computed vertical displacement V before crack initiation - ELS sample
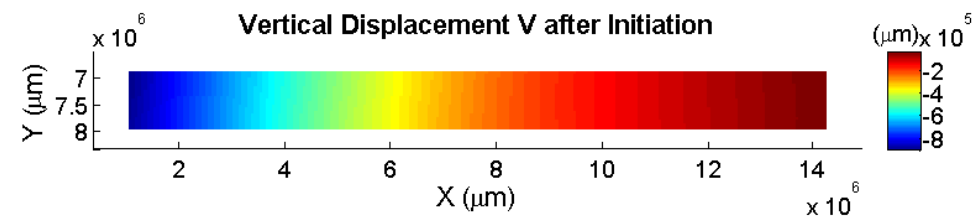
Figure 4.37: Computed horizontal displacement V after crack initiation - ELS sample

Figure 4.38: Frame before initiation (a). Frame after initiation (b).

$\gamma = 1.8$ **Sample**

The mode mixity obtained with global partitioning is $G_{II}/G = 0.8$ (Williams, 1988) while with local partitioning $G_{II}/G = 0.46$ (Suo & Hutchinson, 1990).

Figure 4.39: Computed E_{xx} strain before crack initiation - $\gamma = 1.8$ sample

Figure 4.40: Computed E_{xx} strain after crack initiation - $\gamma = 1.8$ sample
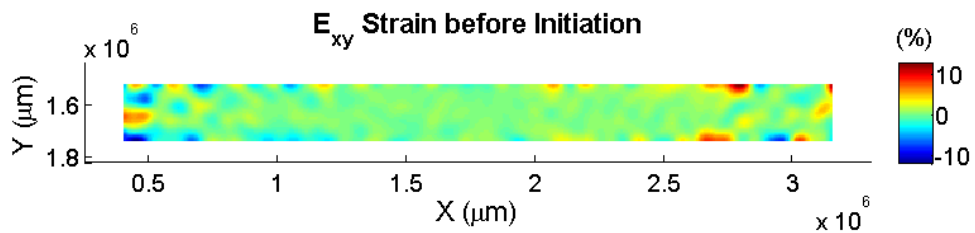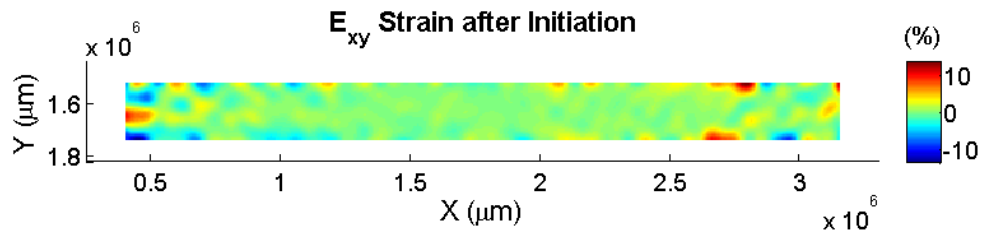

Figure 4.41: Computed E_{xy} strain before crack initiation - $\gamma = 1.8$ sample

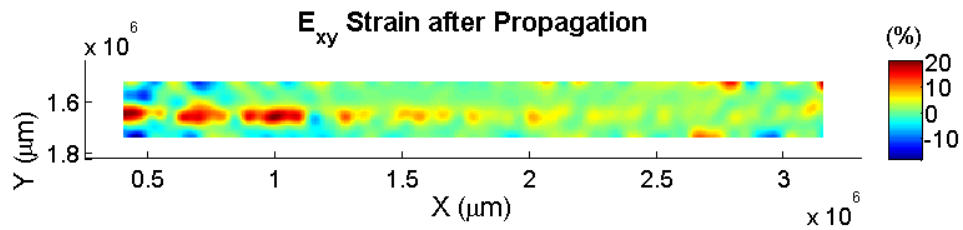Figure 4.42: Computed E_{xy} strain after crack initiation - $\gamma = 1.8$ sample

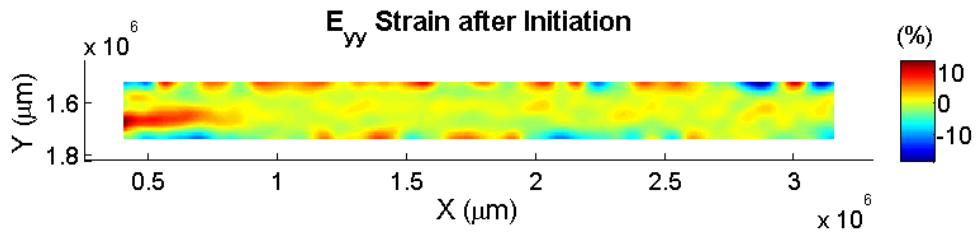Figure 4.43: Computed E_{xy} strain after crack propagation - $\gamma = 1.8$ sample

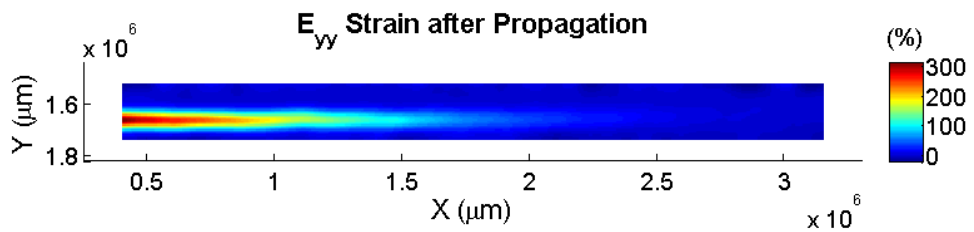Figure 4.44: Computed E_{yy} strain after crack initiation - $\gamma = 1.8$ sample

Figure 4.45: Computed E_{yy} strain after crack propagation - $\gamma = 1.8$ sample
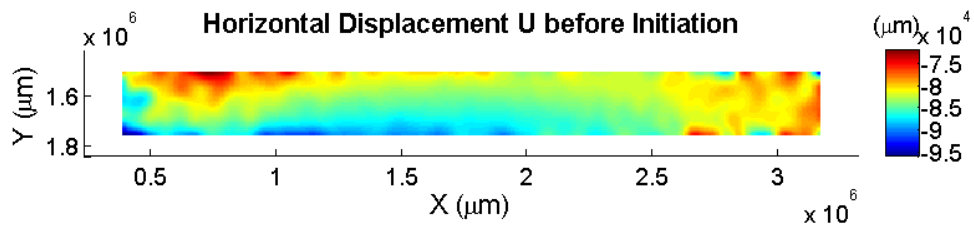
Figure 4.46: Computed horizontal displacement U before crack initiation - $\gamma = 1.8$ sample
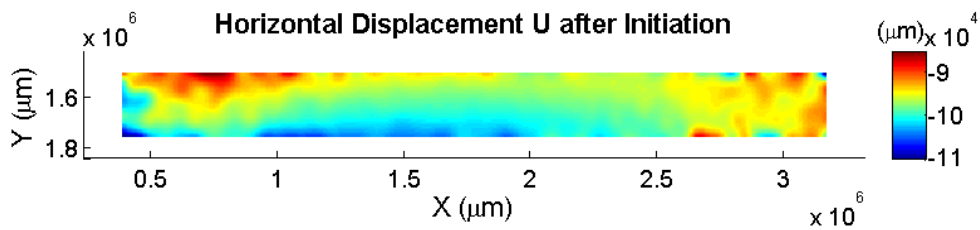

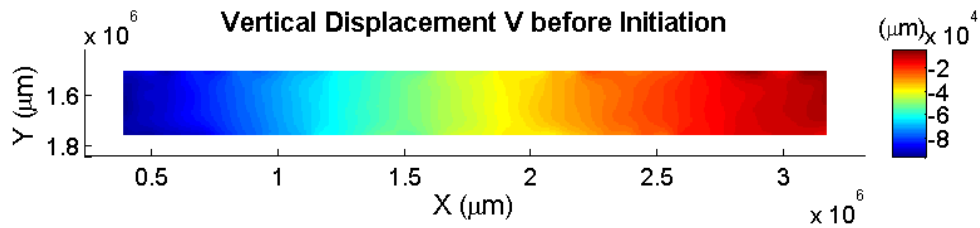Figure 4.47: Computed horizontal displacement U after crack initiation - $\gamma = 1.8$ sample

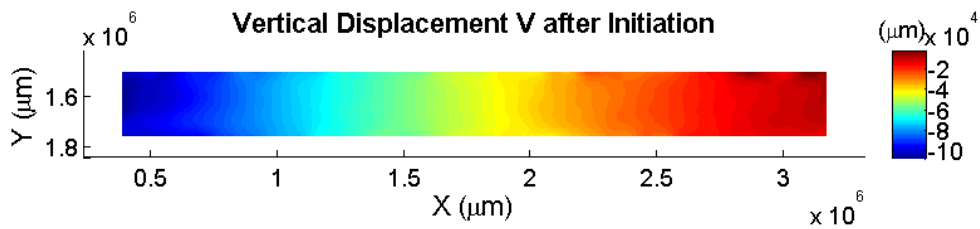Figure 4.48: Computed vertical displacement V before crack initiation - $\gamma = 1.8$ sample

Figure 4.49: Computed vertical displacement V after crack initiation - $\gamma = 1.8$ sample
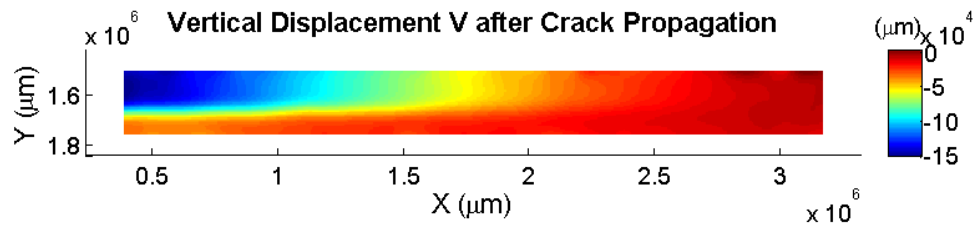
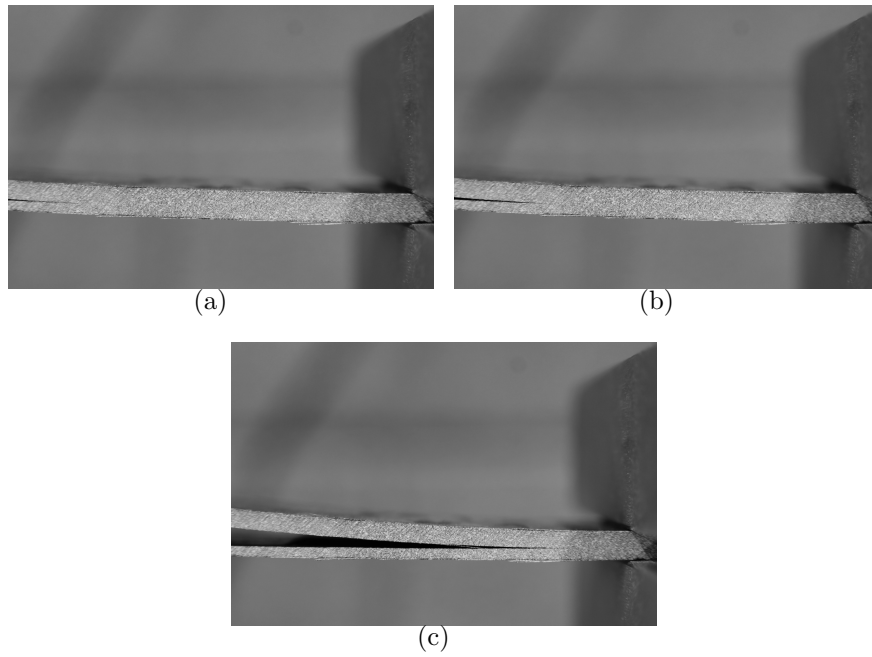Figure 4.50: Computed vertical displacement V after crack propagation - $\gamma = 1.8$ sample

Figure 4.51: Frame before initiation (a). Frame after initiation (b). Frame after propagation (c).

$\gamma = 0.47$ **Sample**

The mode mixity obtained with global partitioning is $G_{II}/G = 0.059$ (Williams, 1988) while with local partitioning $G_{II}/G = 0.4$ (Suo & Hutchinson, 1990).
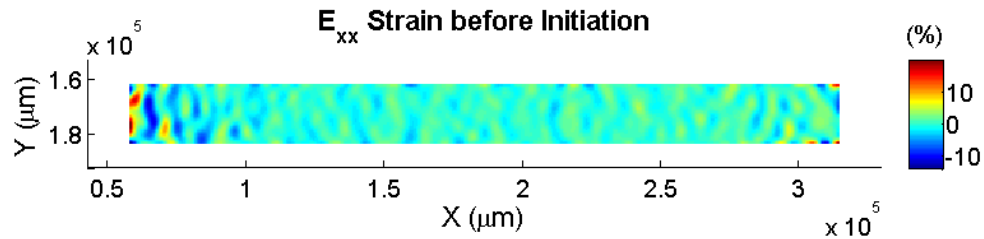

Figure 4.52: Computed E_{xx} strain before crack initiation - $\gamma = 0.47$ sample

Figure 4.53: Computed E_{xx} strain after crack initiation - $\gamma = 0.47$ sample

Figure 4.54: Computed E_{xy} strain before crack initiation - $\gamma = 0.47$ sample
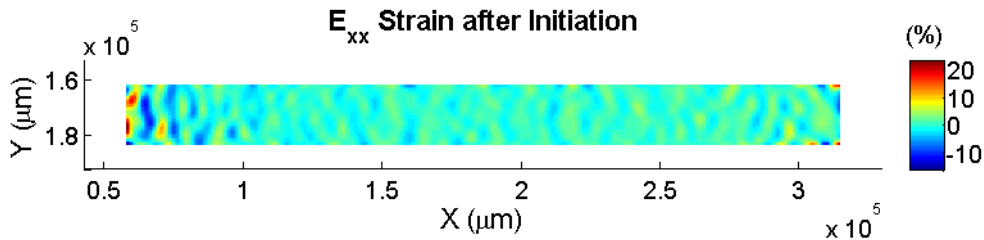

Figure 4.55: Computed E_{xy} strain after crack initiation - $\gamma = 0.47$ sample
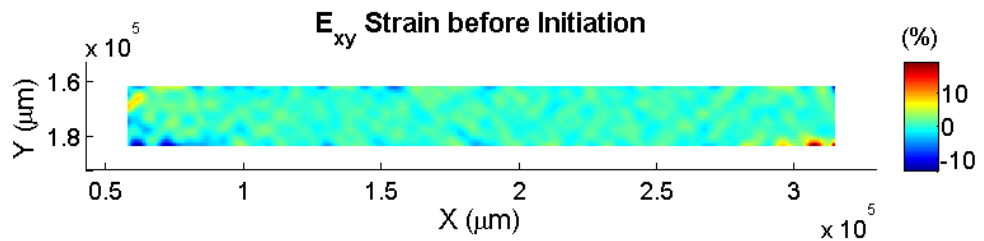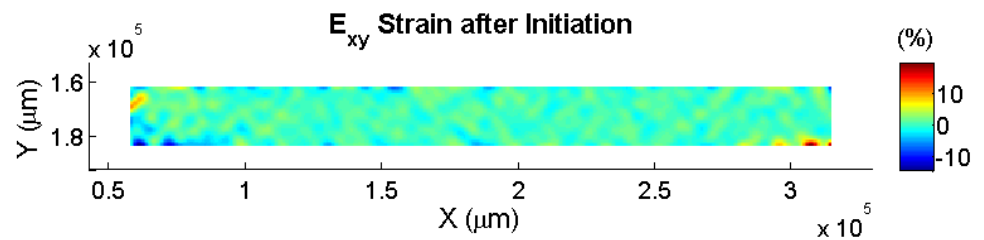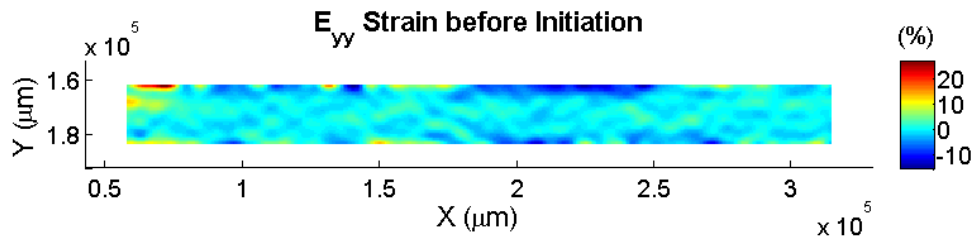
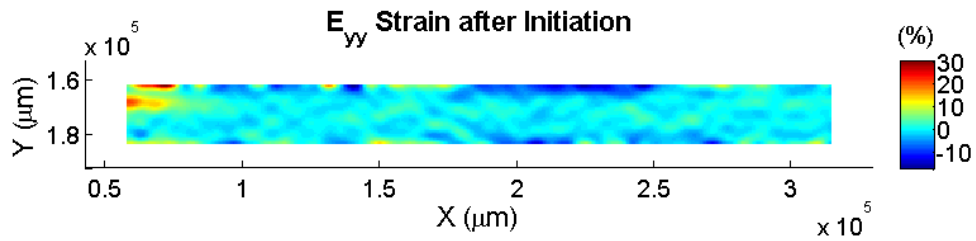Figure 4.56: Computed E_{yy} strain before crack initiation - $\gamma = 0.47$ sample

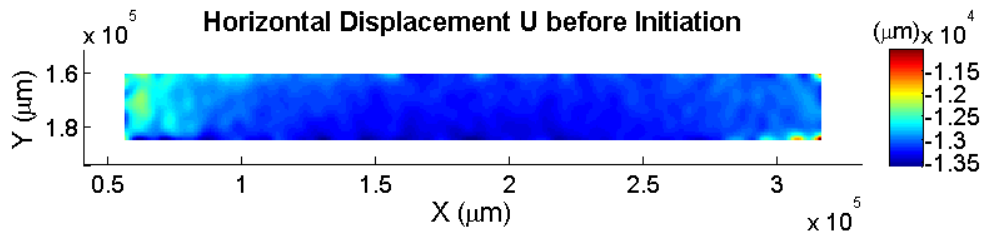Figure 4.57: Computed E_{yy} strain after crack initiation - $\gamma = 0.47$ sample

Figure 4.58: Computed horizontal displacement U before crack initiation - $\gamma = 0.47$ sample
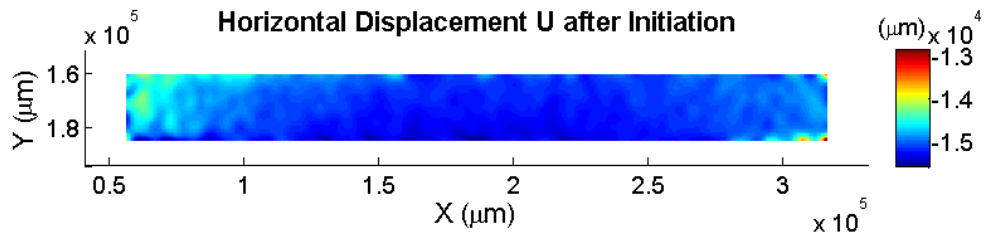
Figure 4.59: Computed horizontal displacement U after crack initiation - $\gamma = 0.47$ sample
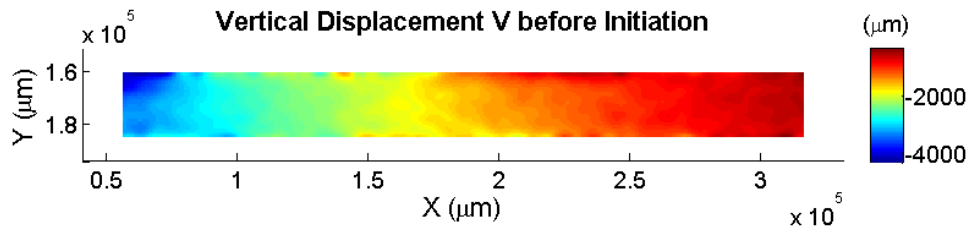
Figure 4.60: Computed vertical displacement V before crack initiation - $\gamma = 0.47$ sample
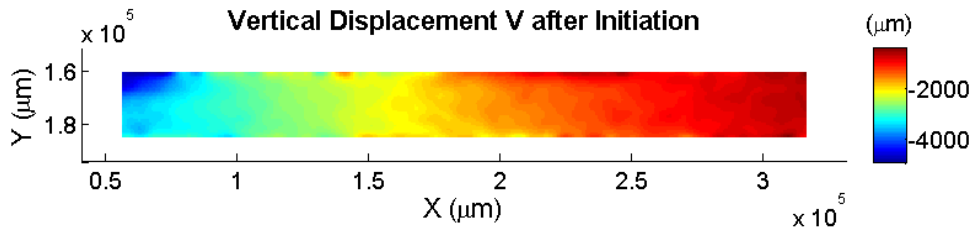
Figure 4.61: Computed vertical displacement V after crack initiation - $\gamma = 0.47$ sample
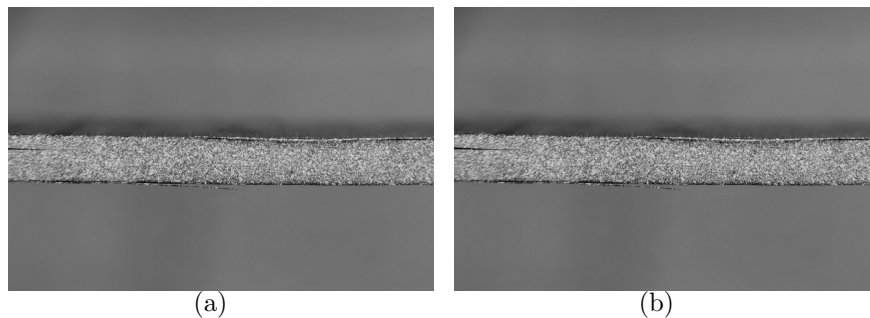
Figure 4.62: Frame before initiation (a). Frame after initiation (b).

4.3   Measuring of Crack Initiation Points

During all of the tests, a load vs. crosshead displacement curve is recorded. From these, initiation points can be read, using the MX/NL point values as described in the standard (ISO 15024:2001).

(a)

(b)
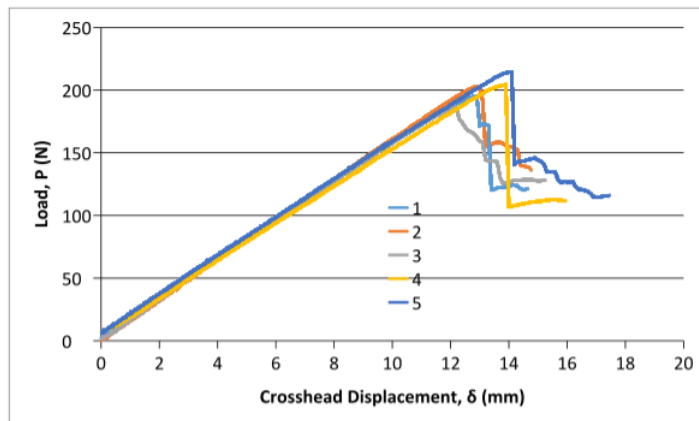
(c)

Figure 4.63: Load vs. crosshead displacement for symmetric samples
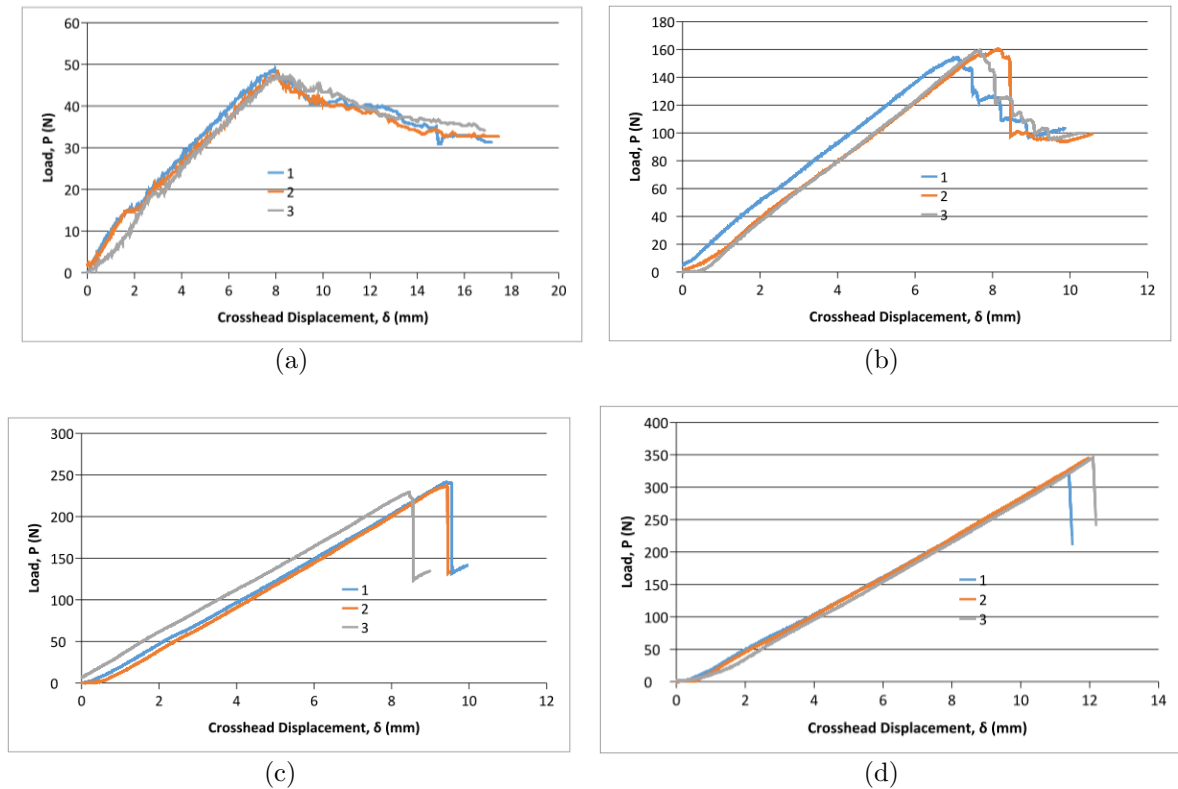
Figure 4.64: Load vs. crosshead displacement for asymmetric fixed ratio mixd mode (AFRMM) samples

It is evident that the initiation values vary significantly depending on the mode mixity, and are about threefold as pure mode I in pure mode II. This corresponds well to previous findings (Conroy, 2015).

The asymmetric tests with high mode II/mode I ratios ($\gamma = 3$ and $\gamma = 4.6$) initiated in a highly unstable manner, where the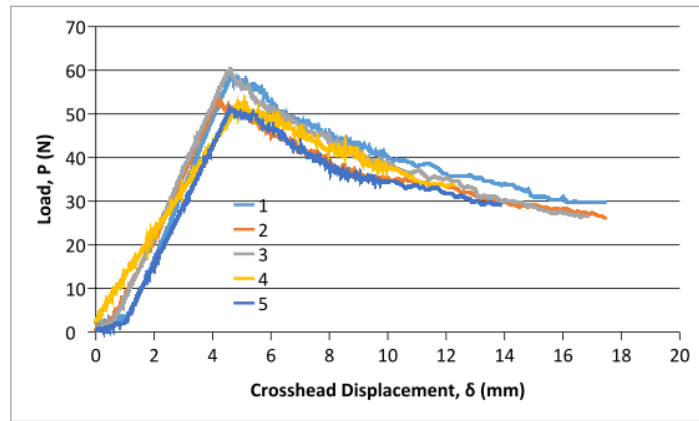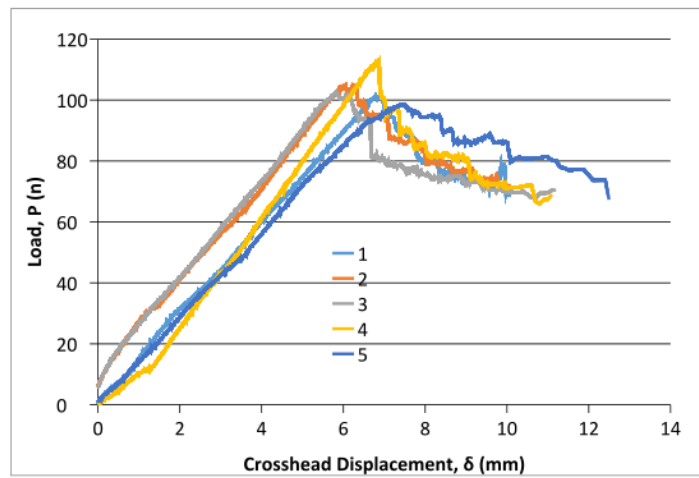 crack propagated through the whole length of the specimens in one instant after being loaded with an unusually high force, in spite of being precracked with two load blocks as with the symmetric samples.

There is a decrease in the initiation values in a mixed mode case close to mode I ($\gamma = 0.47$). This has been observed before, for instance by Dillard et.al. (ISO 15024:2001). In Figure 4.65, experimental data by Conroy is plotted in comparison to various failure criteria.

Figure 4.65: Experimental data compared to failure criteria, showing the drop in toughness close to mode I (Conroy, 2015)

Chapter 5

Conclusion

The present work shows an experimental investigation of mixed mode fracture toughness of unidirectional carbon fibre epoxy resin. The subset size used for most of the correlations was of the order of 100 pixels, as further reduction of the size led to poor co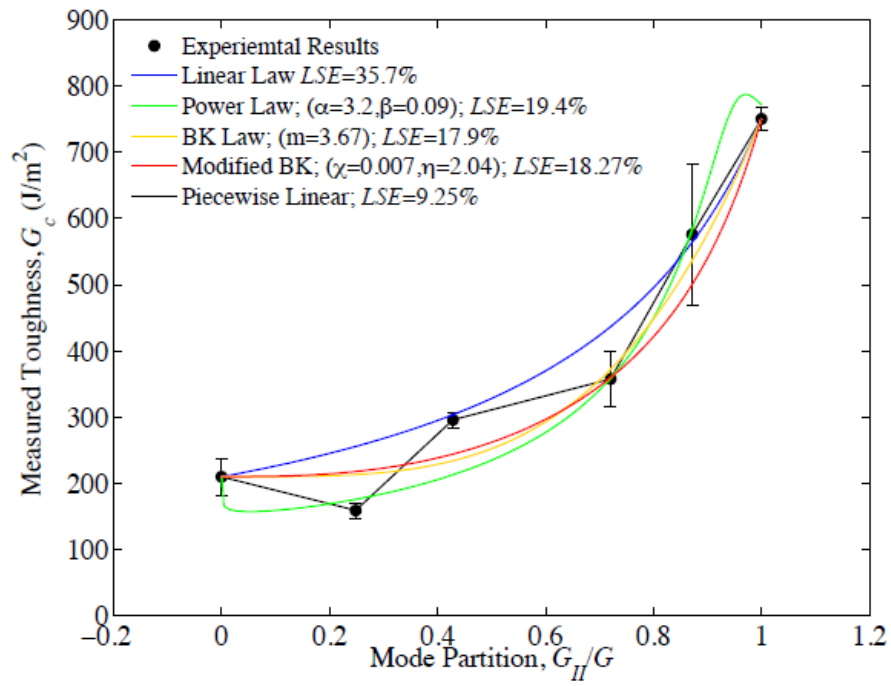rrelated regions and missing data where there were large displacements. The step size was 10 pixels according to recommendation. It is visible that the displacements correlated well, especially the vertical displacements shown on the reference grid show accordance to the the experiment, but not clear enough to be integrated for further computation. The results on the deformed grid shown for the DCB samples display regions of large strains between the beams that are nonexistent in physical reality, as there is no material in this region. It is visible that in parts of computed images there is considerable noise and what looks like numerical diffusion, which is probably due to the large subset size. To obtain images that could correlate using a smaller subset size, the following propositions could be considered:

- using a finer speckle size

- using a macro lens to zoom in on the crack region more closely

- achieving a higher contrast in the photos by using better lighting or a higher ISO sensitivity setting (which also leads to a longer exposure time and lower frame rate)

References

(2016). www.thermwood.comcomposite_fabrication_applications.htm, [Accessed: 08-03-2016].

(2016). Hexcel 8552/as4 material data sheet. http://www.hexcel.com/Resources/DataSheets/Prepreg-Data-Sheets/8552_eu.pdf, [Accessed: 28-02-2016].

ANDERSON, T. (2005). *Fracture Mechanics: Fundamentals and Applications*. Taylor and Francis, 3rd edn.

BLACKMAN, B., BRUNNER, A. & DAVIES, P. (2001). Delamination fracture of continuous fibre composites: Mixed-mode fracture. In D. Moore, A. Pavan & J. Williams, eds., *Fracture Mechanics Testing Methods for Polymers, Adhesives and Composites*, 225–270, Elsevier Science, Amsterdam.

CONROY, M. (2015). *Mixed Mode Fracture in Fibre Reinforced Polymer Composites*. Ph.D. thesis, University College Dublin.

COTTERELL, B. & RICE, J. (1980). Slightly curved or kinked cracks. *Journal of Adhesion Science and Technology*, 155–169.

DILLARD, D., SINGH, H., POHLIT, D. & STARBUCK, J. (2009). Observations of Decreased Fracture Toughness for Mixed Mode Fracture Testing of Adhesively Bonded Joints. *Journal of Adhesion Science and Technology*, 1515–1530.

GAO-11-849 (2011). Aviation Saftey: Status of FAAs Actions to Oversee the Safety of Composite Airplanes. Tech. rep.

GORDON, J. (1991). *The New Science of Strong Materials: Or Why You Don't Fall Through the Floor*. Penguin Books Limited.

ISO 15024:2001 (2001). Fibre-reinforced plastic composites Determination of mode I interlaminar fracture toughness, GIC, for unidirectionally reinforced materials. Tech. rep.

ISO 15114:2014 (2014). Fibre-reinforced plastic composites Determination of the mode II fracture resistance for unidirectionally reinforced materials using the calibrated end-loaded split (C-ELS) test and an efective crack length approach. Tech. rep.

JONES, E.M.C. (2013). Documentation for Matlab-based DIC code.

JONES, R.M. (1998). *Mechanics Of Composite Materials*. Materials Science and Engineering Series. Taylor and Francis.

MOHAN, J. (2010). *An Investigation of Composite-to-Composite Bonding*. Ph.D. thesis, University College Dublin.

MURPHY, N. (2015). Fracture Mechanics.

QUAN, D. & IVANKOVIĆ, A. (2015). Efect of coreshell rubber (CSR) nano-particles on mechanical properties and fracture toughness of an epoxy polymer. *Polymer*, **66**.

SUO, Z. & HUTCHINSON, J. (1990). Interface crack between two elastic layers. *International Journal of Fracture*, 1–18.

WILLIAMS, J. (1988). On the calculation of energy release rates for cracked laminates. *International Journal of Fracture*, 101–119.